Molecular Neurobiology (2019) 56:748–760
https://doi.org/10.1007/s12035-018-1127-4

Stem Cells from Human Exfoliated Deciduous Teeth Modulate Early Astrocyte Response after Spinal Cord Contusion

Fabrício Nicola[1,2] · Marília Rossato Marques[1,2] · Felipe Odorcyk[1,2] · Letícia Petenuzzo[2] · Dirceu Aristimunha[2] · Adriana Vizuete[2] · Eduardo Farias Sanches[2] · Daniela Pavulack Pereira[3] · Natasha Maurmann[3,4] · Carlos-Alberto Gonçalves[2] · Patricia Pranke[3,4,5] · Carlos Alexandre Netto[2]

Received: 25 February 2018 / Accepted: 11 May 2018 / Published online: 24 May 2018

Abstract

The transplantation of stem cells from human exfoliated deciduous teeth (SHED) has been studied as a possible treatment strategy for spinal cord injuries (SCIs) due to its potential for promoting tissue protection and functional recovery. The aim of the present study was to investigate the effects of the early transplantation of SHED on glial scar formation and astrocytic reaction after an experimental model of SCI. Wistar rats were spinalized using the NYU Impactor. Animals were randomly distributed into three groups: control (naive) (animal with no manipulation); SCI (receiving laminectomy followed by SCI and treated with vehicle), and SHED (SCI rat treated with intraspinal SHED transplantation, 1 h after SCI). In vitro investigation demonstrated that SHED were able to express mesenchymal stem cells, vimentin and S100B markers, related with neural progenitor and glial cells, respectively. The acute SHED transplantation promoted functional recovery, measured as from the first week after spinal cord contusion by Basso, Beattie, and Bresnahan scale. Twenty-four and 48 h after lesion, flow cytometry revealed a spinal cord vimentin$^+$ cells increment in the SHED group. The increase of vimentin$^+$ cells was confirmed by immunofluorescence. Moreover, the bioavailability of astrocytic proteins such as S100B and Kir4.1 shown to be increased in the spinal cord of SHED group, whereas there was a glial scar reduction, as indicated by ELISA and Western blot techniques. The presented results support that SHED act as a neuroprotector agent after transplantation, probably through paracrine signaling to reduce glial scar formation, inducing tissue plasticity and functional recovery.

Keywords Spinal cord injury · Human dental pulp stem cells · Glial scar formation · Progenitor cells

Abbreviations

APC	Allophycocyanin
AQP4	Aquaporin 4
BBB	Basso, Beattie, and Bresnahan scale
FITC	Fluorescein isothiocyanate
GFAP	Glial fibrillary acidic protein
Kir	Inward rectifying potassium channel
MASCIS	Multicenter Animal Spinal Cord Injury Study
MSCs	Mesenchymal stem cells
PE	Phycoerythrin
PMSF	Phenylmethyl-sulphonyl fluoride
SCI	Spinal cord injury
SHED	Stem cells from human exfoliated deciduous teeth
S100B	Calcium-binding protein
TBS	Tris-buffered saline
Tx	Triton X-100
Vimentin	Progenitor neural cells
βIII-tubulin	Neuronal microtubule protein

✉ Fabrício Nicola
fabricionicola@hotmail.com

[1] Post Graduate Program in Neuroscience, Universidade Federal do Rio Grande do Sul, Porto Alegre, Brazil

[2] Department of Biochemistry, Institute of Basic Health Sciences, Universidade Federal do Rio Grande do Sul, R. Ramiro Barcelos, 2600 anexo, Porto Alegre, Rio Grande do Sul 90035-003, Brazil

[3] Hematology and Stem Cell Laboratory, Universidade Federal do Rio Grande do Sul, Porto Alegre, Brazil

[4] Post Graduate Program in Physiology, Universidade Federal do Rio Grande do Sul, Porto Alegre, Brazil

[5] Stem Cell Research Institute, Porto Alegre, Brazil

Introduction

Spinal cord injury (SCI) is an incapacitating condition that disconnects axons from neuronal cells causing functional deficits,

such as the loss of voluntary movements and sensation; its worldwide incidence is 10 to 49 individuals per million [1]. The primary injury is caused by traumatic spinal cord damage, which is difficult to be prevented or treated [2]; after this, a cascade of events known as secondary injury will destroy neurons that were not damaged in the primary event [3]. Cell death caused by spinal cord injury involves neurons, glial cells, and progenitor cells present in the spinal cord [4–6]. These events are mediated mainly by microglial cells, which regulate inflammation and phagocyte debris, and by astrocytes, which proliferate and act in the formation of the glial scar [7, 8]. The natural replacement of progenitor cells after spinal cord lesion leads to the production of new glial cells, which can be considered a potential therapeutic target [6].

Astrocyte proliferation and migration can be seen as from 72 h after the injury [5] and the characteristic astrocyte hypertrophy is a consequence of the increased expression of intermediate filaments, such as the glial fibrillary acidic protein (GFAP), a process called reactive astrocytosis or astrogliosis [9, 10]. Astrocytes bear unique and dynamic cytoarchitecture and phenotypic features activated by changes in the microenvironment. They express a wide range of receptors and ion channels that, interconnected with glial cells and neurons, regulate the water transport across membranes in response to osmotic gradients by the water aquaporin 4 channel [11–13], or by buffering the potassium ion through Kir 4.1, an inward rectifying potassium channel (Kir), which removes potassium from extracellular medium [14–17]. Along with this, astrocytes can also stimulate cell proliferation, migration, and differentiation via the production and release of calcium-binding protein B (S100B) [18, 19].

Stem cells from human exfoliated deciduous teeth (SHED) are self-renewing mesenchymal stem cells (MSCs), found within the perivascular niche of the dental pulp [20, 21], have been shown to reduce the secondary damage and the early neuronal death [5, 22] and to promote functional recovery after engrafting into lesioned spinal cord [23–25]. Such effects have been suggested to involve paracrine mechanisms that activate endogenous tissue repairing pathways [24–26]. Previous reports show the involvement of SHED in the secretion of proteins which regulate the phenotype of macrophage cells [26], as well as the reduction of early inflammatory response and apoptosis, resulting in long-term motor neurons survival/preservation [5].

The present study was designed to verify the effects of SHED transplantation, 1 h after spinal cord contusion, on tissue astrocyte reaction and on precursor cell proliferation in the acute phase of lesion; in addition, the potential of SHED to express neural, glial, and precursor proteins in the in vitro phase was studied. The working hypothesis is that SHED will express glial and precursor cell proteins in vitro and that, after transplantation, they will reduce the early hypertrophy of astrocytes and stimulate the presence of progenitor cells in the spinal cord of injured rats.

Experimental Procedure

Isolation and Cultivation of SHED

Stem cells from human exfoliated deciduous teeth (SHED) were collected, isolated, and cultivated in accordance with the protocol of Bernardi and colleagues [27]. The donor gave written informed consent to participate in the study, which was approved by the Ethics Committee of the Universidade Federal do Rio Grande do Sul (#296/08).

The dental pulp was removed and incubated at 37 °C for 60 min in buffer with 300,000 U/mg of type 1 colagenase (Gibco, USA). Dental pulp cells were removed from the dental parenchyma and cultivated, as previously described [28]. All the pulp tissue was removed (crown and root) from the dentin and the resulting cell suspension was seeded with a density of 5×10^3 cells/cm^2. The culture medium used was DMEM (Dulbecco's modified Eagle's medium) low glucose, supplemented with 10% fetal bovine serum (Cultilab, Brazil) and 1% penicilin/estreptomicin (Sigma-Aldrich®, USA). The medium was changed and repeated every 3 or 4 days, thereafter. A passage using trypsin-EDTA 0.05% (Sigma-Aldrich, USA) was performed when confluence was reached to loosen the cells from the plate. Cells between the 4th and 10th passage were utilized for culture characterization analysis and for cell transplantation.

Characterization of SHED

The cells were suspended in PBS at 10^6 cells from human exfoliated teeth ($n = 3$) and incubated for 30 min with the following conjugated antibodies against human cell surface molecules: CD29, CD34, CD90, and CD105 (hematopoietic stem/progenitor cells/endothelium), CD44, CD45, CD73 (common leukocyte antigens), CD14 (monocyte/macrophage), and CD184 (stromal cell surface marker), conjugated with fluorescein isothiocyanate (FITC), phycoerythrin (PE), or allophycocyanin (APC) from BD (Becton Dickinson, USA) as previously reported (Nicola et al., 2016; Maurmann et al. 2017). Data acquisition was performed using the FACSAria III flow cytometer (BD Biosciences, USA), and 10,000 events were analyzed using FACS Diva 6.1.3 software (BD Biosciences, USA) (Bernardi et al., 2011; Nicola et al., 2016; Maurmann et al. 2017).

SHED differentiation in mesenchymal cell types was tested to confirm the identity of the population obtained. Assays for osteogenic, adipogenic, and chondrogenic differentiation were performed following protocols already described [29]. For osteogenic differentiation, cell cultivation was carried out for about 21 days in a medium containing SFB (15%), dexamethasone (0.1 μM), ascorbic acid 2-phosphate (50 μM), and β-glycerophosphate (15 mM). The deposition of mineralized matrix was observed by staining with Alizarin Red S at

pH 4.2. For adipogenic differentiation, cell cultivation was carried out for about 30 days in DMEM medium containing 10% of SFB, 3-isobutyl-1-methylxanthine (IBMX) (0.5 mM), dexamethasone (1 μM), insulin (1.74 μM), indomethacin (50 μM), and rosiglitazone (1 μM). Adipocytes were identified by observation of fat droplets under phase contrast microscopy and staining with Oil Red O. For chondrogenic differentiation, the adherent cells were cultivated in differentiation medium for 30 days. The medium was comprised of DMEM supplemented with SFB (10%), dexamethasone (0.1 μM), 1× ITS (0.01 mg/mL recombinant human insulin, 5.5 μg/mL human transferrin, and 5 ng/mL sodium), TGF-α1 (10 ng/mL), and AsAP (50 μM). Chondrogenesis was demonstrated by Alcian Blue staining.

All culture media were changed every 3–4 days and when differentiated, the cells were washed with phosphate buffer, fixed with 4% paraformaldehyde, and washed with Milli-Q water, and finally, the specific staining was performed.

Experimental Design

Male Wistar rats aged 2 months (200–250 g body weight) were obtained from the Animal House of the Instituto de Ciências Básicas da Saúde of the Universidade Federal do Rio Grande do Sul. They were maintained in a temperature-controlled room (21 ± 2 °C) on a 12/12 h light/dark cycle, with food and water available ad libitum. All procedures were in accordance with the Guide for the Care and Use of Laboratory Animals adopted by the National Institute of Health (USA) and with the Federation of Brazilian Societies for Experimental Biology. The study was approved by the Research Ethics Committee of the University (#26116). The animals were randomly divided into three experimental groups: naive (without any manipulation), SCI (laminectomy followed by SCI and treated with vehicle), and SHEDs (SCI treated with SHEDs). Three experiments were run: (1) in vitro phase, for the SHED characterization ($n = 3$ cultures); (2) in vivo, for the functional evaluation of hind limbs by BBB scale ($n = 5$–7 per group); (3) in vivo, spinal cord samples were collected 6, 24, and 48 h after lesion in order to perform ELISA for GFAP and S100B and flow cytometry to quantify the vimentin$^+$ cells and Western blot analysis of AQP4 and Kir4.1 ($n = 7$–8 per group). Naive rats were used as controls, aiming to reduce the number of experimental animals. There was a 10% death rate after the surgical procedure. Animal care was in accordance with the Multicenter Animal Spinal Cord Injury Study (MASCIS) protocols (Fig. 1) [30].

Spinal Cord Injury and SHED Transplantation

The animals were previously anesthetized with a mixture of xylasine (100–150 mg/kg) and ketamine (60–90 mg/kg). Laminectomy was performed at the 9th thoracic vertebra (T9) level, and injury was induced through the drop of a 10 g weight from 25 mm height by the use of New York University Impactor device (NYU-Impactor®; W.M. Keck Center for Collaborative Neuroscience, USA) [23, 31]. The SHED group received the administration of 3×10^5 cells diluted in 0.9% NaCl. Cell suspension (10 μL) was added at the lesion site, 1 h after the injury with a 25-μL sterile Hamilton syringe and carried out without immunosuppression [32]. The animals were sutured following the surgical procedure and housed in individual cages; bladder evacuation was performed daily until function was restored. Antibiotic (Enrofloxacino, Bayer, Brazil; 6 mg/kg) was administered for 7 days after the procedure to prevent infection.

Motor Function Assessment

The Basso, Beatie, and Bresnahan scale (BBB) was used to evaluate the motor function of rats' hind limbs after their spontaneous behavior in an open field has been recorded. The BBB assesses the hind limb motor function with scores ranging from 0, complete paralysis, to 21, normal locomotion [33]. Evaluation began 2 days before the surgery and was repeated 2 days after, and then weekly until the sixth week after SCI. Two examiners who were blind to the animal's treatments observed the video recording for scale scoring [33].

ELISA for GFAP

The spinal cords were homogenized in PBS (50 mM NaCl, 18 mM Na_2HPO_4, 83 mM $NaH_2PO_4 \cdot H_2O$, pH 7.4), containing 1 mM of EGTA and 1 mM of phenylmethylsulphonyl fluoride (PMSF). Microtiter plates (96-well flat-bottom) were coated overnight at 4 °C with 100 μL of Tris-buffered saline (TBS) containing 70 μg of protein. The plates were then washed three times with Tween-20/TBS (0.05%) and blocked with bovine serum albumin (2%) for 2 h at room temperature. After blocking, anti-GFAP antibody (polyclonal anti-GFAP rabbit antibody, diluted 1:1000) was incubated for 2 h at room temperature in albumin/TBS (0.5%). After washing with Tween-20/TBS (0.05%), a second incubation with peroxidase-conjugated anti-rabbit, diluted 1:1000, was carried out for 1 h at room temperature. Peroxidase substrate (Sigma Fast OPD) was added and incubated for 30 min in the dark after washing twice with Tween-20/TBS (0.05%) and once with TBS. The reaction was stopped by the addition of 3NHCl (50 μL), and the absorbance was read at 492 nm on a Microtiter plate reader (Tecan-Spectra, Japan). The standard GFAP curve ranged from 0.1 to 10 ng/mL [34]. Results were expressed as % of naive.

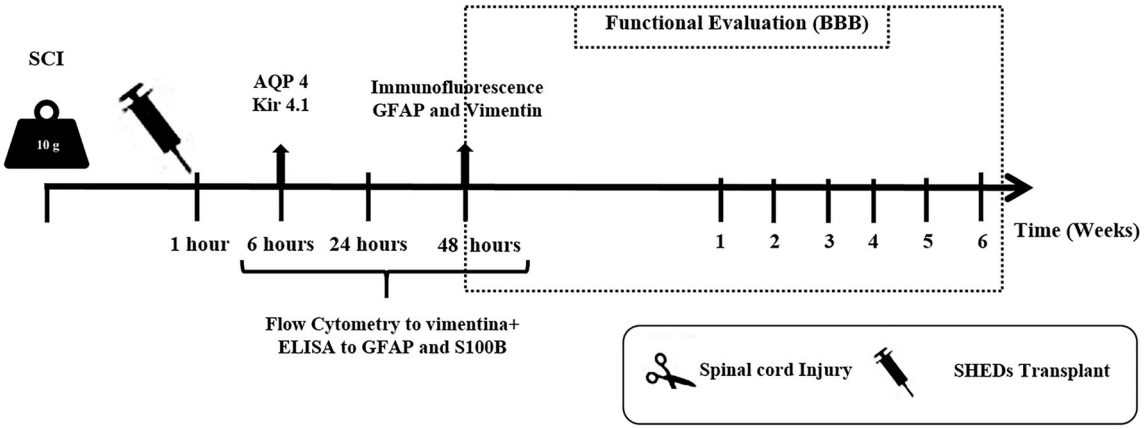

Fig. 1 Experimental design of in vivo experiments. The spinal cord injury was performed in two groups: SCI and SHED. The SHED group received cell administration 1 h after lesion. In the first experiment, the animals were functionally evaluated 48 h and weekly after SCI. In the second experiment, samples of the spinal cords were collected 6, 24, and 48 h after lesion to evaluate the number of vimentin^{+} cells and the expression of GFAP and S100B proteins. Six hours after contusion, Western blot was performed to AQP4 and Kir 4.1, and 48 h after injury, immunofluorescence to GFAP and vimentin was run in the samples of spinal cords

ELISA for S100B

The spinal cords were homogenized in PBS (50 mM NaCl, 18 mM Na_2HPO_4, 83 mM $NaH_2PO_4{\cdot}H_2O$, pH 7.4), containing 1 mM of EGTA and 1 mM of phenylmethyl-sulphonyl fluoride (PMSF). The plates were previously coated overnight at 4 °C with 100 μL of a fresh 1/1000 dilution of monoclonal anti-S100B in 50 mM of carbonate–bicarbonate buffer (pH 9.5). The plates were washed three times with 200 μL of washing buffer (0.1% BSA in PBS containing 0.05% Tween-20). The samples were incubated with blocking solution (2% BSA, 150 μL) for 1 h at room temperature, and then, the plates were washed once with 200 μL of washing buffer. Following this, 50 mM of Tris buffer (pH 8.6) containing 50 μL of samples (diluted with PBS containing 0.2% BSA) or standard curve (range from 0.0019 to 1 ng/mL) were incubated for 2 h at 37 °C on a warming plate. The plates were washed three times with 200 μL of washing buffer. Polyclonal anti-S100B antibody (diluted 1/5000 in 0.5% BSA - 100 μL) was incubated for 30 min at 37 °C. The plates were washed three times with washing buffer (200 μL), and after, 100 μL of anti-rabbit peroxidase-conjugated diluted 1/5000 in 0.5% BSA were incubated for 30 min at 37 °C. The plates were washed three times with 200 μL of washing buffer and once with PBS (200 μL). The samples were incubated with 200 μL of a fresh solution of Sigma Fast OPD in the dark, for 30 min at room temperature. A quantity of 50 μL of 3 M HCl was added, and the microplates were read at 492 nm. The standard S100B curve ranged from 0.02 to 1 ng/ml. Results were expressed as % of naive [35].

Flow Cytometry Analysis

The spinal cords were dissociated with Trypsin/PBS (0.006 g/mL) (Sigma-Aldrich - T2600000), and the cells were then permeabilized with 0.1% PBS Triton X-100 (Tx) for 10 min at room temperature and blocked for 15 min with 3% normal goat serum (Sigma-Aldrich - G9023). After blocking, the cells were incubated with the primary antibody against vimentin (Mouse, Sigma Aldrich – V2258), at a final concentration of 1:100, at room temperature for 2 h. The cells were washed twice with PBS and incubated for 1 h with IgG antibody Alexa-fluor 488 anti-mouse at a final concentration of 1:200. Negative controls were included for setting up the machine voltages and to determine the negative region of dot plot. The emission of fluorochrome was recorded through a specific band-pass fluorescence filter: green (FL-1; 488 nm long pass). Fluorescence emission was collected using logarithmic amplification. Data from 10,000 events (intact cells) were acquired and the number of cells was determined after exclusion of debris events from the dataset. The number of cells in each quadrant was computed, and cells stained separately were expressed as the percentage of positive immune labeled cells [36]. All flow cytometric acquisitions and analyses were performed using FACSCalibur (Becton Dickinson, Franklin Lakes, NJ, USA) and Flow Jo software v10.1 [5, 37].

Immunofluorescence

In vitro, plates with SHED were washed with PBS and permeabilized with PBS-Tx (0.25%), and then blocked with albumin (1%) for 30 min. The following primary antibodies against neuronal microtubule βIII-tubulin protein (rabbit IgG, 1:200, Abcam - ab18207); glial fibrillary acidic protein GFAP (mouse IgG, 1:200, Sigma Aldrich - G3893); progenitor neural cells vimentin (mouse, 1:100, Abcam - ab8978), and calcium-binding protein S100B (mouse, 1:200 Sigma Aldrich - AMAB91038) were used. This procedure was carried out in PBS-Tx containing 1% of albumin at 4 °C for 24 h. Following the PBS washes, sections were incubated with

secondary antibody anti-mouse Alexa 488 (1:500, Molecular Probes, Invitrogen, USA) or secondary antibody anti-rabbit Alexa 555 (1:500, Molecular Probes, Invitrogen, USA). A laser scanning confocal microscope (Olympus FV 1000, Japan) was used for the visualization of fluorescent labeling.

In vivo, the animals were anesthetized with pentobarbital (100 mg/kg, i.p.; Cristália, Brazil) followed by transcardiac perfusion with 0.9% saline and then with 4% paraformaldehyde (Reagen, Brazil) in 0.1 M phosphate buffer (PBS, pH 7.4). The spinal cord was removed from C5 to L5 in the thoracic region, post-fixed in the same fixative solution and cryoprotected with 15 and 30% sucrose diluted in phosphate buffer saline (PBS). After cryoprotection, the samples were frozen and cooled in liquid nitrogen until slicing [5]. The thoracic region of the spinal cord was transversally cut into 20 μm sections in cryostat (Leica, Germany). The slices were washed with PBS, permeabilized in PBS-Tx (0.25%) and then blocked with albumin (1%) for 30 min. Primary antibodies against glial fibrillary acidic protein GFAP (rabbit IgG, 1:200, Sigma Aldrich - SAB4300647) and against progenitor neural cells vimentin (mouse, 1:100, Abcam - ab8978) were used. This procedure was carried out in PBS-Tx containing 1% of albumin at 4 °C for 24 h. Following the PBS washes, the sections were incubated with secondary antibody anti-mouse Alexa 555 (1:500, Molecular Probes, Invitrogen, USA) or secondary antibody anti-rabbit Alexa 488 (1:500, Molecular Probes, Invitrogen, USA). The slices were covered in aqueous mounting medium (FluorSave, Calbiochem, Germany) and coverslipped. Laser scanning confocal microscope (Olympus FV 1000, Japan) was used for the visualization of fluorescent labeling.

Quantitative image analysis of GFAP staining intensities was performed in transversal slices, where the larger cavity area (epicenter) was found and five slices above and five slices below the epicenter (10 slices per animal) were assessed, for six animals per group. To reduce the variability between the interest areas, the GFAP intensity was always quantified in the ventral white matter (VWM); all analyses were made using high magnification images (× 20). An area of interest (AOI) was determined (8.460 μm^2) to assess the staining intensity. The integrated density value per unit of area was obtained through the capture and analysis of images in the software Image J v. 1.46. Data are reported as the mean of integrated densities/mm^2, as previously described [23].

Western Blotting

Tissue was homogenized in lysis buffer containing 50 mM of Tris-HCl, 4% of SDS, and 2 mM of EDTA; it was boiled and received 25% of a solution containing β-mercaptoethanol (5%), glycerol (40%), and bromophenol blue (0.02%). The proteins were analyzed, using equal amounts of 20 μg, through 4–12% SDS-PAGE (Mini-PROTEAN, Bio-Rad – 1658004) and subsequently transferred to nitrocellulose membrane (Trans-blot SD semi-dry transfer cell, Bio-Rad – 1703940) for 1 h in transfer buffer (48 mM Trizma, 39 mM glycine, 20% methanol). The nitrocellulose membranes were washed for 10 min in TBS (0.5 M NaCl, 30 mM Trizma, pH 7.5), followed by incubation overnight at 4 °C in a blocking solution (TBS plus 2% bovine serum albumin and 0.05% Tween 20). After incubation, the blot was washed three times for 5 min with TBS plus 0.05% Tween-20 (T-TBS) and then incubated overnight at 4 °C in blocking solution containing the primary antibodies at a final dilution of 1:1000. The primary antibodies used were as follows: AQP4 (Rabbit, Millipore - AB3594) and Kir4.1 (Goat, Santa Cruz - sc-23637). The blot was then washed three times for 5 min with T-TBS and incubated for 1 h in a solution containing peroxidase conjugated with anti-rabbit IgG (GE Life Sciences - RPN4301) or anti-goat IgG (Abcam - AB6741) diluted 1:10000. The blot was washed again three times for 10 min with T-TBS and once for 10 min with TBS. The chemiluminescence signal was detected using an ECL Kit (GE Life Sciences - RPN2109). Immunoblots were quantified by scanning the membranes in ImageQuant LAS4000 (GE Healthcare Life Sciences, UK) and determining optical densities through Image Studio Lite V5.0 (LI-COR Biosciences, USA). The results were expressed as the ratio of intensity of the protein of interest to that of anti-β-actin from the same membrane.

Statistical Analysis

Data are presented as mean ± standard error of the mean (SEM). One-way ANOVA was used to analyze quantitative data, followed by Duncan post hoc test to reveal differences between the groups whenever indicated. The Student's *t* test was used for comparison between two groups. Significance was assumed at $P < 0.05$. All analyses were carried out using IBM SPSS Statistics software v.19.

Results

In Vitro SHED Characteristics

The SHED showed the ability to adhere to the plastic their morphology was similar to that of fibroblasts. Furthermore, they also demonstrated comparable trilineage differentiation into chondrocytes, osteocytes, and adipocytes when exposed to appropriate differentiation media. After the differentiation period, the cells produced fat droplets, stained red in the interior of the cells, characterizing adipocytes (Fig. 2a, b); glycosaminoglycans, stained in blue, accompanied by a change in cell

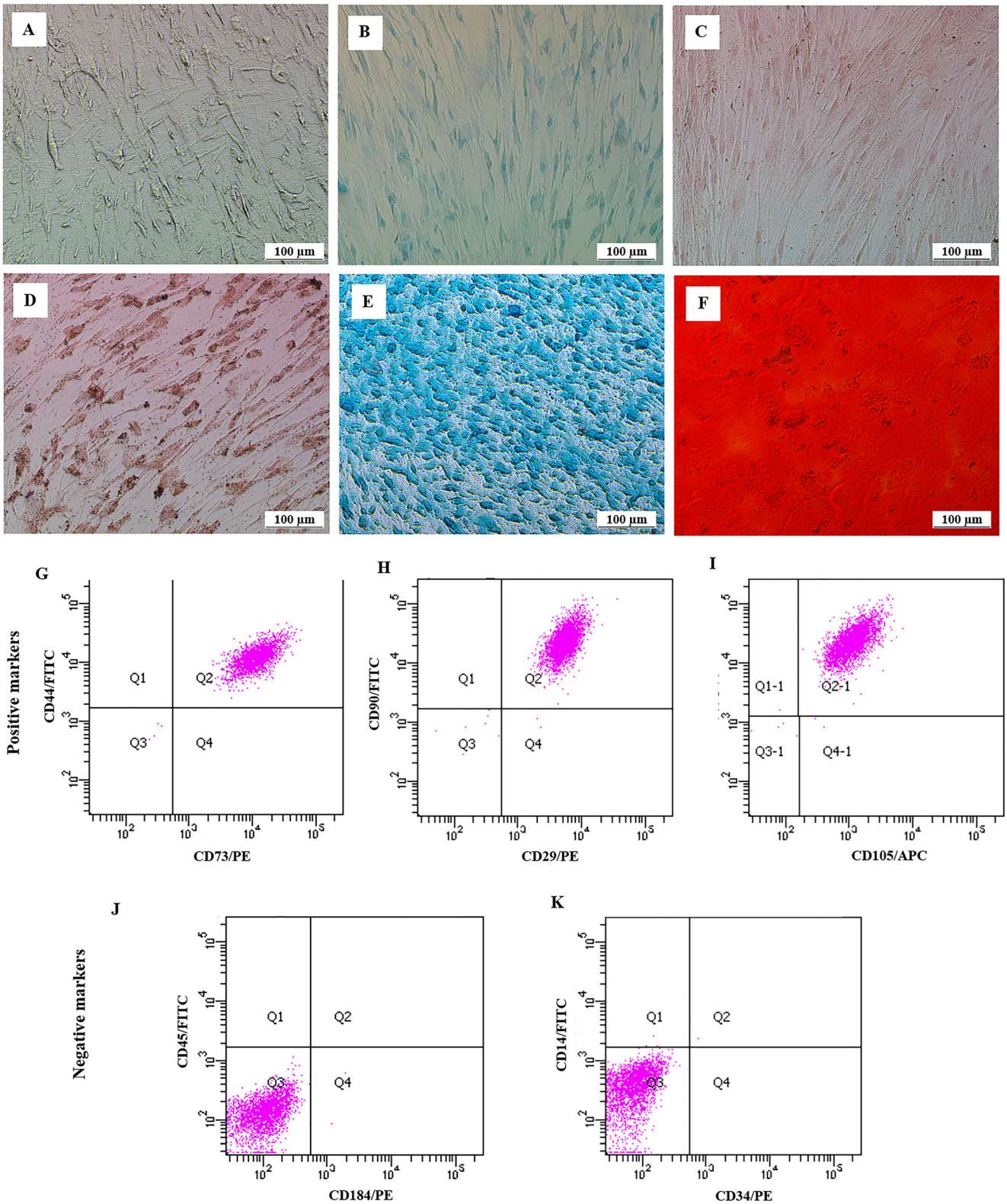

Fig. 2 Characterization of SHED. Microphotographs of cell differentiation. **a** Adipogenic control. **b** Chondrogenic control. **c** Osteogenic control. **d** Adipogenic differentiation. **e** Chondrogenic differentiation. **f** Osteogenic differentiation. The scale corresponds to 100 µm. Immunophenotypic characterization of SHED by flow cytometry. They were positive (> 99.5%) for CD44 and CD73 (**g**), CD90 and CD29 (**h**), CD105 (**i**). There was low expression (< 2%) for CD34 (**j**) and CD184 (**k**)

morphology, showing chondrocytes characteristics (Fig. 2b, e); and bone matrix, stained red on the outside of the cells (Fig. 2c, f). The immunophenotypic analysis of the primary culture of SHED showed positivity for CD29 (99.8%), CD90 (99.7%), CD105 (99.7%), CD44 (99.8%), and CD73 (99.8%) (Fig. 2g–i). On the other hand, SHED showed low expression to hematopoietic markers CD14 (0.1%), CD34 (< 0.1%), CD184 (0.1%), and CD45 (< 0.1%) (Fig. 2j, k).

Immunofluorescence analysis was run to verify the phenotype of SHED for specific proteins in the culture phase. As depicted in Fig. 3, SHED did not express neuronal protein βIII-tubulin nor astrocyte's GFAP; however, they expressed vimentin, a protein of quiescent neural progenitors and astrocytes, as well as S100B, which is found in astrocytes and oligodendrocytes.

Functional Response

Behavioral assessment by the use of the BBB Locomotor Rating Scale was conducted 2 days before, 2 days after and weekly until the sixth week post-contusion. In the preoperative assessment, all animals showed normal locomotor function; however, hind limb function of SCI and SHED was greatly impaired 2 days after the injury, as compared to the control group (Fig. 4). Spontaneous motor function recovery was observed in both lesioned groups ($P < 0.05$, Fig. 4) as from 7 days after injury. In the SHED group, a further significant increment of hind limb function was seen as early as one-week post lesion; such effect, remained until the sixth week. The control group remained with maximum scores in all assessments, i.e., presented normal motor function.

Spinal Cord Vimentin$^+$ Cells

Vimentin$^+$ cells were quantified six, 24 and 48 h after spinal cord lesion to quantify the progenitor cells. There was an increase of vimentin$^+$ cells in the spinal cord 6 h after the injury in the SCI group (2.35 ± 0.17% of vimentin$^+$ cells) and in the SHED group (1.85 ± 0.17% of vimentin$^+$ cells), as compared to the naive rats (0.86 ± 0.08% of vimentin$^+$ cells) (Fig. 5) [$F(2.16) = 23.31$, $P < 0.05$]. SHED presented an increase in the number of vimentin$^+$ cells in the spinal cord tissue (2.64 ± 0.15% of vimentin$^+$ cells and 2.26 ± 0.12% of vimentin$^+$ cells) 24 and 48 h after lesion. It is suggested that SHED either increased the cell proliferation of the vimentin$^+$ cells or induced the vimentin protein expression in the cells that were not expressing it before, or both.

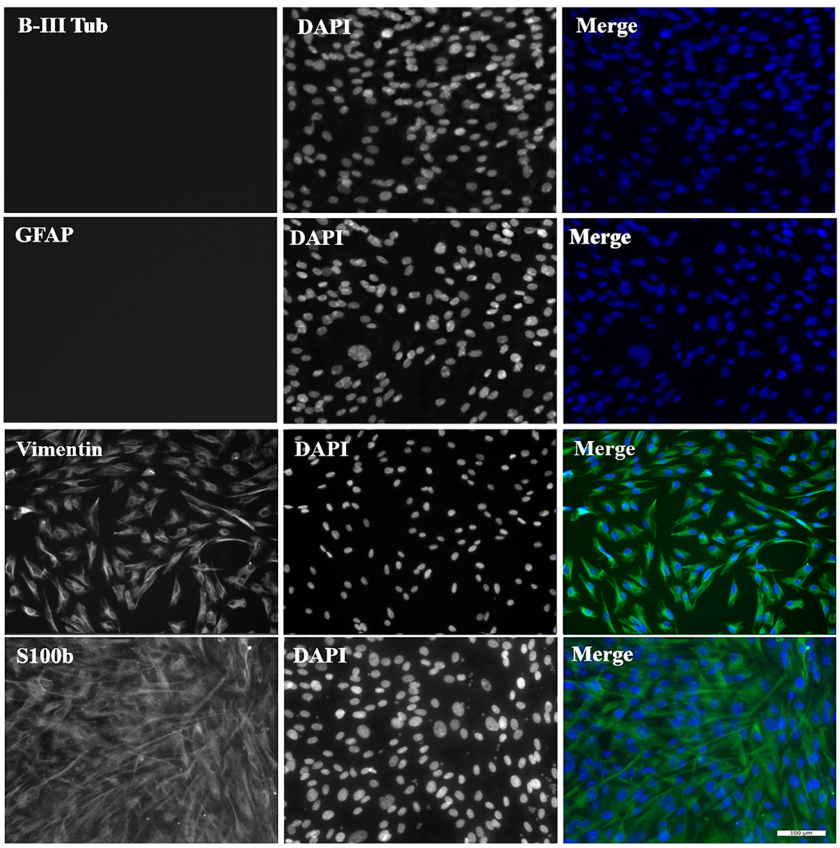

Fig. 3 Immunofluorescence of SHED primary culture. Microphotographs of SHED for the mature neuronal marker (βIII-tubulin), the astrocyte marker (GFAP), the precursor neural marker (vimentin), and the calcium-binding protein marker (S100B). The scale corresponds to 100 μm

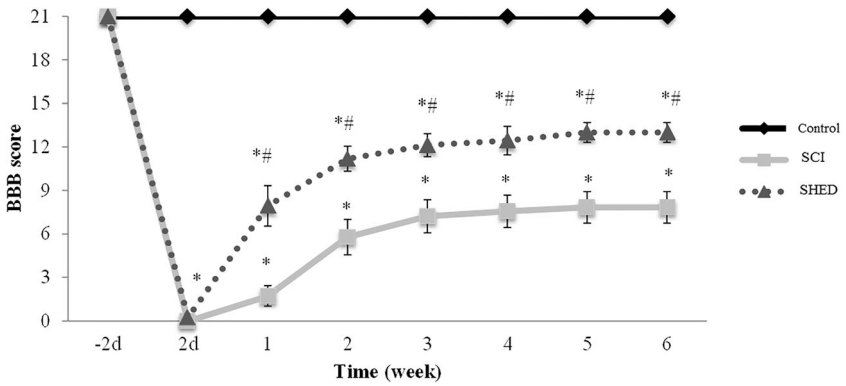

Fig. 4 Hind limbs function after spinal cord contusion assessed through the Basso, Beatie, and Bresnahan scale (BBB). Data expressed as mean ± SE of BBB scores. *Difference from the control group. #Difference from SCI group

GFAP and S100B Expression

The ELISA analysis to evaluate the GFAP and S100B expression in spinal cord tissue was run 6, 24, and 48 h after lesion. Six hours after lesion, the SCI (32 ± 11.76% of GFAP expression) and the SHED groups (49.92 ± 7.10% of GFAP expression) had reduced expression of GFAP in comparison to the naive group (100 ± 13.71% of GFAP expression) (Fig. 6a) [$F(2.19) = 5.00$, $P < 0.05$]. A further loss of GFAP was evidenced 24 h in both spinalized groups, SCI (50.55 ± 8.21% of GFAP expression) and SHED (60.74 ± 8.21% of GFAP expression) (Fig. 6a) [$F(2.19) = 4.10$, $P < 0.05$]. Interestingly, SCI caused an increase of GFAP expression 48 h after lesion, reaching 264.04 ± 37.38% of GFAP expression, while the SHED group (170.04 ± 15.20% of GFAP expression) did not differ from the naive rats (100.00 ± 28.28% of GFAP expression) (Fig. 6a) [$F(2.19) = 8.27$, $P < 0.05$]. The early over expression of this protein was reduced by SHED, suggesting that the transplanted cells were able to prevent, or reduce, astrocytic hypertrophy.

S100B expression was reduced only 24 hafter lesion in the SCI group (76.16 ± 1.55% of S100B expression) [$F(2.18) = 3.60$, $P < 0.05$] and 48 h in the SHED group (69.35 ± 5.28% of S100B expression) (Fig. 6b) [$F(2.18) = 6.68$, $P < 0.05$]. This result suggests that SHED was able to delay the reduction of S100B as evidenced 24 h after SCI.

Immunofluorescence of GFAP and Vimentin

The immunofluorescence was performed in the ventral white matter of the SCI and SHED groups to confirm the presence of vimentin$^+$ and GFAP$^+$ cells 48 h after lesion. As evidenced by ELISA, in the immunofluorescence, there was a reduction of GFAP expression in the SHED group (85.62 ± 9.81 intensity/mm^2) when compared with the SCI (144.12 ± 12.38 intensity/mm^2) [$t(11) = 3.70$, $P < 0.05$] (Fig. 7). The SHED group presented vimentin$^+$ cells without GFAP co-expression, vimentin$^+$ cells co-expressing GFAP and GFAP$^+$ cells only (Fig. 8). In the SCI group, the number of vimentin$^+$ cells were lower than in the SHED group, and all vimentin$^+$ cells were co-expressed with GFAP.

Astrocyte AQP4 and Kir4.1 Expression

The contents of AQP4 and Kir4.1 were studied 6 h after spinal cord injury by Western blot (Fig. 9a). The AQP4 expression was significantly reduced in both SCI (82.72 ± 12.89% of control) and SHED (82.52 ± 1.67% of control) groups (Fig. 9b) [$F(2.12) = 3.90$, $P < 0.05$]. Interestingly, the Kir4.1 expression remained at the control levels in the SCI group (104.33 ± 34.27% of control) while SHED transplantation caused an increase of expression (158.37 ± 30.12% of control) (Fig. 9c) [$F(2.13) = 5.48$, $P < 0.05$]. These results indicate that SHED

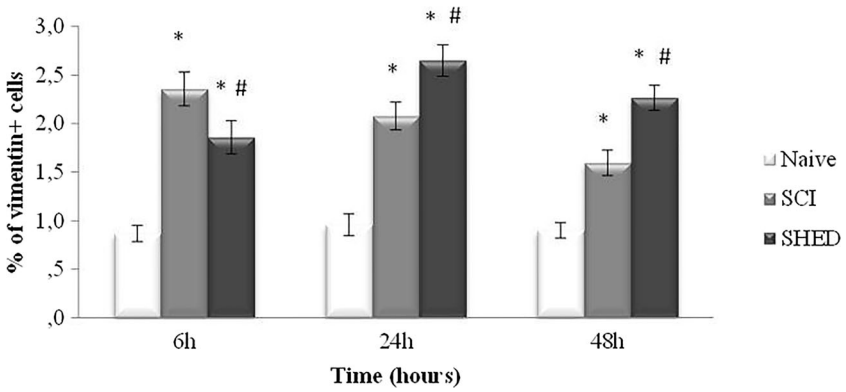

Fig. 5 Flow cytometry of vimentin$^+$ cells at 6, 24, and 48 h after spinal cord lesion to naive, SCI, and SHED experimental groups. Data expressed as mean ± SE. *Difference from the naive group, $p < 0.05$. #Difference from the SCI group, $P < 0.05$ ($n = 7$–8 per group)

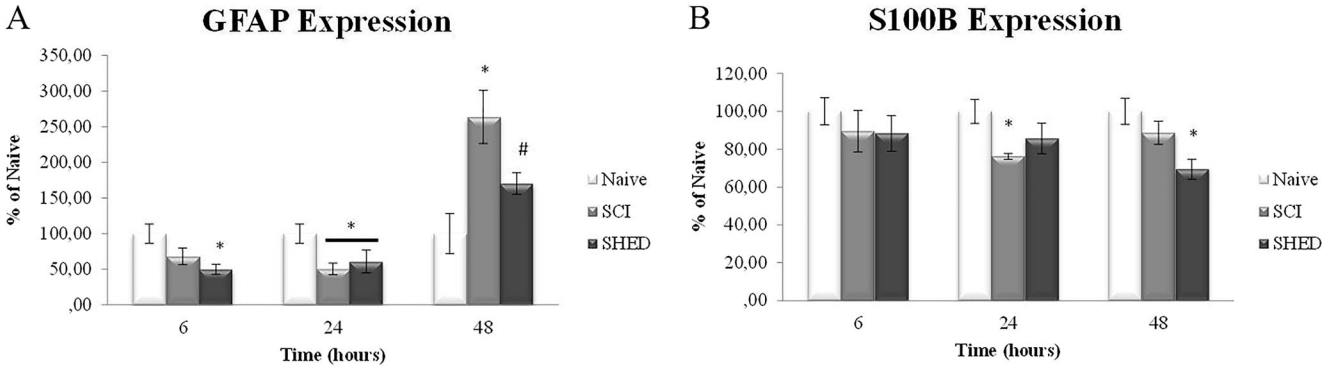

Fig. 6 ELISA of GFAP (**a**) and S100B (**b**) expression in naive, SCI, and SHED groups, run 6, 24, and 48 h after spinal cord lesion. Data expressed as mean ± SE. *Difference from the naive group, $P < 0.05$. #Difference from the SCI group, $P < 0.05$ ($n = 7–8$ per group)

transplantation, although not affecting AQP4, the main brain water channel, caused an increase in the expression of the inward rectifier potassium channel Kir4.1.

Discussion

The effects of SHED transplantation on tissue astrocytic cells in the acute phase of spinal cord injury were assessed, beginning just 7 h after the injury. Before transplantation, the primary cultivated SHED demonstrated mesenchymal stem cell characteristics and expressed proteins related with autocrine and paracrine signaling (S100B) and neural progenitor cells (vimentin). It is the first description of early parenchyma protection against the astrocytic hypertrophy as from 48 h after SHED transplantation, which could be regulated by the reduction delay of calcium-binding protein S100B between 24 and 48 h. Interestingly, it also favored the increment of progenitor cells in the spinal cord of treated animals, evidenced by the increment of vimentin$^+$ cells that remained at least until 48 h. Astrocytic cells were shown to be modified after SHED transplantation, by an increase of inward rectifying potassium channel Kir4.1 expression. Along with these molecular effects, the SHED promoted a long-lasting functional recovery that started in the first week after transplantation.

In the in vitro phase, SHED express proteins related to neuroprotection, axonal elongation and neural progenitor cells [24–26]. The expression of vimentin, a cytoskeletal component found in immature neural cells [38], by SHED, shows that these cells may be capable of differentiating into neuronal-like cells. Another protein found by immunofluorescence was S100B, corroborating with previous report which confirmed the presence of S100B in the SHED by flow cytometry [24]. S100B is secreted or released from astrocytes and has double trophic and toxic effects on neurons, astrocytes and microglia, depending on the levels of concentration present in the analyzed tissue [18, 39]. More studies are needed to support the idea that transplanted SHED produces and releases acceptable levels of S100B to promote positive tissue modifications in the environmental conditions of lesion. Although the cells expressed a progenitor (vimentin) and a signaling protein (S100B), they were not able to express

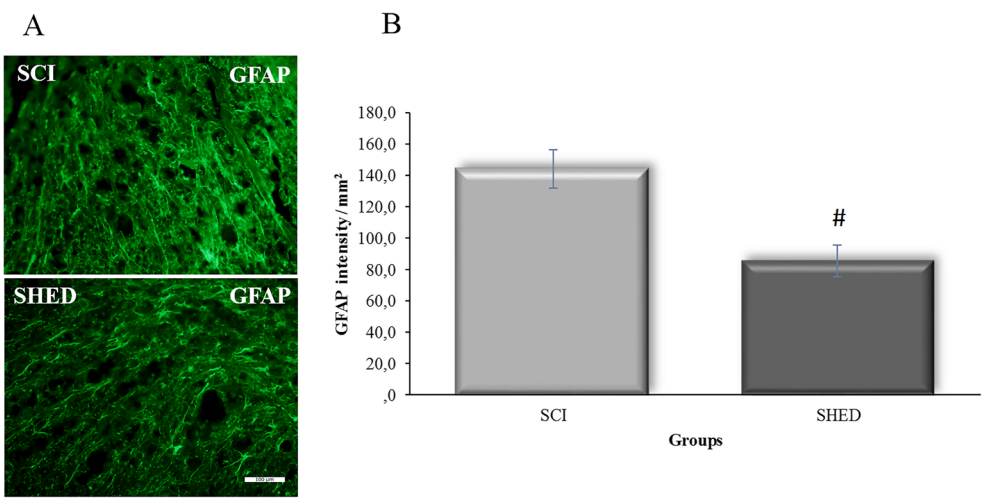

Fig. 7 Representative GFAP immunostaining in the ventral white matter of spinal cord, 48 h after the spinal cord injury (SCI), in SCI and SHED groups (**a**). Densitometry of GFAP (**b**). Data are expressed as mean ± SE. #Difference from the SCI group, $P < 0.05$ ($n = 7–8$ per group). The scale corresponds to 100 μm

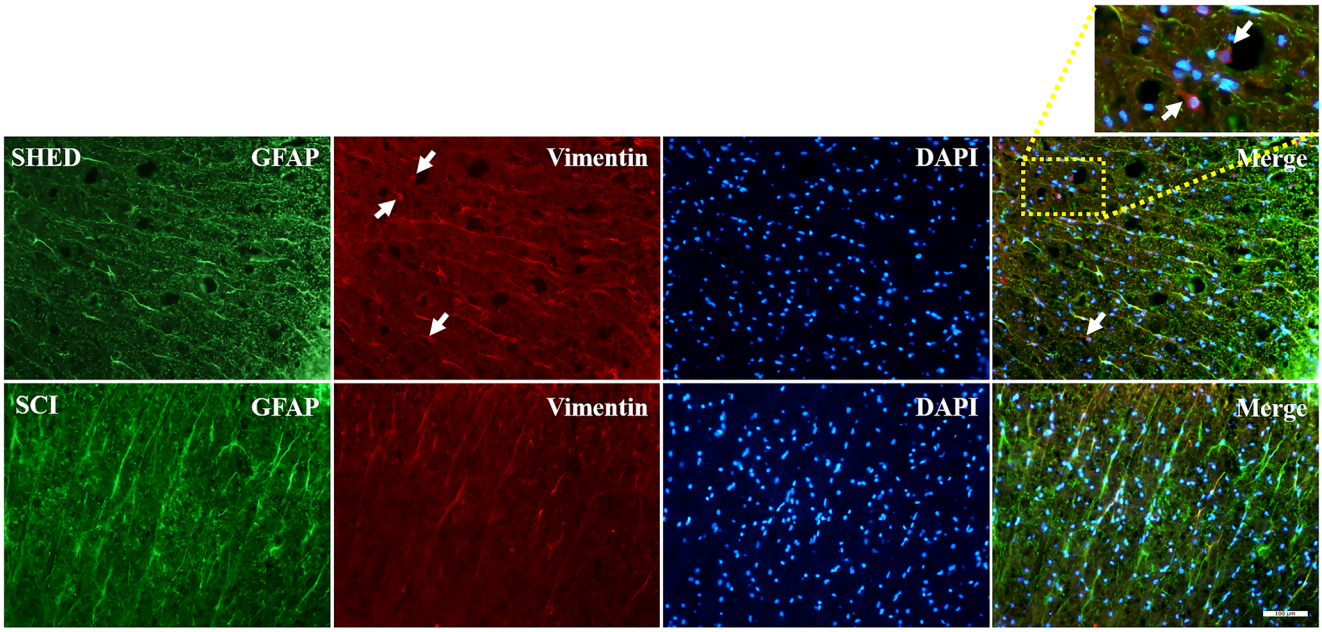

Fig. 8 Immunofluorescence of GFAP and vimentin in the ventral white matter of SCI and SHED groups. The arrows highlight vimentin^{+} cells without double labeling with GFAP. The scale corresponds to 100 μm

GFAP and βIII-tubulin, proteins related with the mature neuronal cells; however, there is controversy in the literature concerning this result [24, 40].

Adult spinal cord presents multiple populations of progenitor cells in the ependymal region and in the parenchyma [6, 41, 42]. In response to a cord lesion, these progenitor cells are

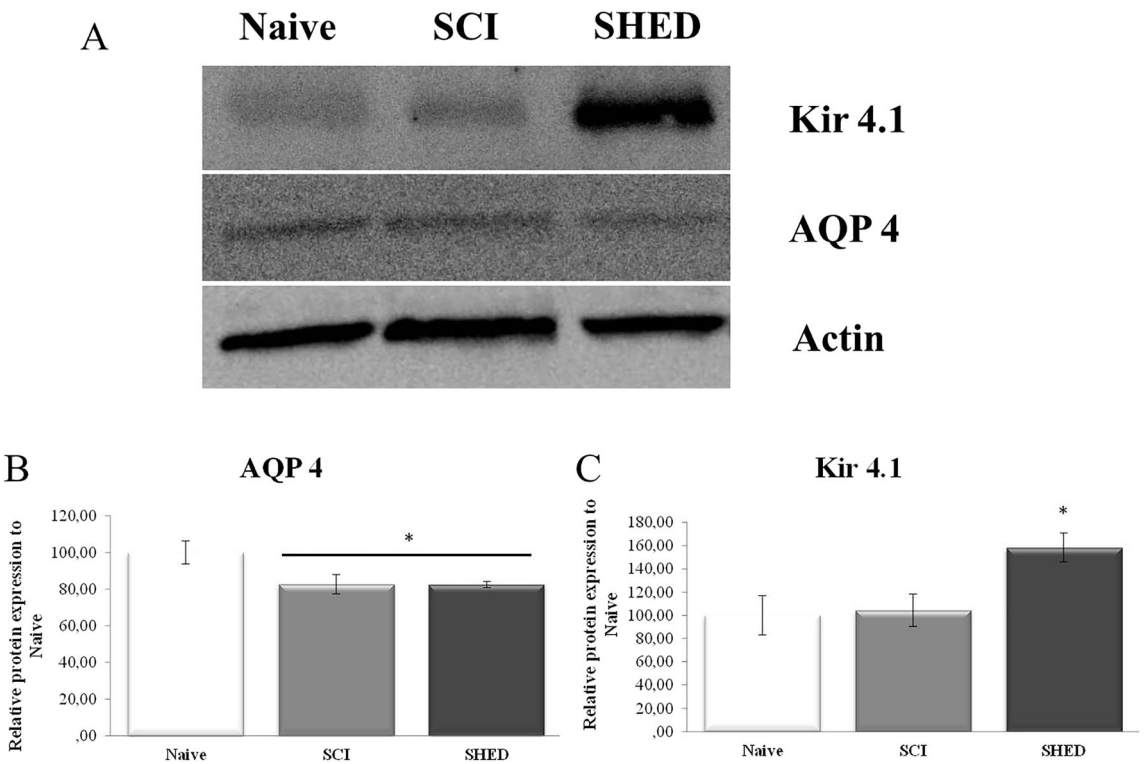

Fig. 9 Western blot analysis of AQP 4 and Kir 4.1 run 6 h after spinal cord injury; naive, SCI, and SHED experimental groups. Representative images of AQP 4 and Kir 4.1 (**a**). Quantification of AQP 4 (**b**) and of Kir 4.1 (**c**). Data expressed as mean ± SE. *Difference from the Naive group, $P < 0.05$ ($n = 7–8$ per group)

rapidly replaced by a second quiescent stem/progenitor population [6], which are suggested as a therapeutic target to stimulate the proliferation [43], aiming to improve the tissue response and functional recovery after spinal contusion [41]. Vimentin is a protein present in quiescent neural progenitor cells and astrocytes [38, 42], which is upregulated after spinal cord injury, and this increase in the adult rodent spinal cord may signify a reversion to an earlier developmental state of these cells, possibly facilitating the axonal growth and plasticity [42]. The number of vimentin^{+} cells was naturally increased 6 h after lesion, remaining in a high number up to 48 h in the SCI group; however, the SHED transplantation showed an increment, besides that verified in the SCI group, from 24 h, which was maintained up to 48 h, which may mean an increase of tissue plasticity.

Spinal cord injury leads to astrocyte proliferation and hypertrophy by GFAP upregulation [5, 44]. Tightly interweaving of astrocytic processes helps in the glial scar formation, which inhibits the neurite outgrowth and restricts axonal regeneration [44–47]. For decades, the reduction of the glial scar has been a goal for SCI treatment [48]; however, their ablation leads to an increase in neurons and oligodendrocyte loss, with reduction of hind limbs motor performance [49]. A reduction of GFAP expression was seen 24 h after lesion, as expected by the natural astrocyte loss at this time [4, 5]. Interestingly, there was an increase of GFAP expression 48 h after lesion, which the transplantation of SHED was able to maintain the GFAP at normal levels. The reduction of GFAP expression after SHED engraft was confirmed in a later phase of spinal cord contusion; it promoted neuronal survival and functional recovery [23, 24]. Therefore, the reduced GFAP expression suggests an early inhibitory action of the SHED on glial scar formation after SCI.

As GFAP, calcium-binding protein (S100B) has been suggested as a good marker for central nervous system damage and SCI [50, 51]. There was a reduction of S100B expression 24 h after lesion, returning to normal levels at 48 h, while in the rats that received SHED transplantation, this S100B decline was reduced within 24 h. The drop in levels was only confirmed at 48 h, when it was observed that they were different from the naive group. A raise of S100B levels occurs only after 72 h [52]; therefore, this reduced decline in S100B levels may signify a tissue signaling contribution or an attempt to reduce the early glial death [5].

Along with GFAP and S100B, key astrocyte proteins, such as the water channel protein aquaporin-4, related to edema [11, 53] and the inward rectifying potassium channel Kir4.1, related to the withdrawal of potassium from the extracellular medium [14, 54], were analyzed 6 h after lesion. The lesion size grows as from 5 min after lesion because the secondary injury, the cystic cavity and edema formation [55]. The cord injury reduces the AQP4 levels in the spinal tissue in the acute phase [56], corroborating with the results here presented. At 6 h, SHED were not able to prevent the loss of AQP4 in the spinal tissue, suggesting no influence of SHED on AQP4, i.e., no interference in the edema formation. Both AQP4 and Kir4.1 may be co-expressed in the central nervous system [57], and a widespread loss of Kir4.1 is expected 7 days after the spinal cord injury [58]. Six hours after injury, the SCI group kept normal levels of Kir4.1 in the spinal cord while SHED provided an increase, i.e., there was probably an inward increase of potassium from the extracellular medium to the intracellular medium of the astrocyte, which favors neuroprotection, as described previously [5, 24] by reducing the neuronal excitability [14].

All tissue modulations previously discussed may have contributed to the main result, which is the functional recovery. As expected, the spinal cord injury produced functional deficits when assessed by the BBB scale [5, 31, 59, 60]. The SHED transplantation accelerated functional recovery as from the first week [23, 26], as depicted in Fig. 4; an improvement which remained significant until the sixth week. This early functional recovery shows the potential of early tissue modifications after SHED transplantation [5, 24, 25, 61].

Conclusion

SHED transplantation in the acute phase after spinal cord contusion promoted an increase of progenitor cells as from 24 h, suggesting an influence in the tissue plasticity after the lesion. Grafted SHED reduced the increase of GFAP expression after 48 h, promoting an early inhibition of glial scar formation; modulating astrocytic proteins, such as S100B, delaying the decrease of levels of this protein; and promoting an increase of Kir4.1, a key protein related to potassium buffering, essential for reducing neuronal excitability. As expected, SHED improved the functional recovery. Taken together, presented results support the idea that SHED act as a neuroprotector agent after transplantation, probably through paracrine signaling and tissue plasticity mechanisms.

Acknowledgements This work was supported by funds from the Conselho Nacional de Desenvolvimento Cientifico e Tecnológico do Brasil (CNPq), Coordenação de Aperfeiçoamento de Pessoal de Nível Superior (CAPES) and Stem Cell Research Institute.

Compliance with Ethical Standards

All procedures were in accordance with the Guide for the Care and Use of Laboratory Animals adopted by the National Institute of Health (USA) and with the Federation of Brazilian Societies for Experimental Biology and with the Brazilian Law for Laboratory Animals care n^{o} 11.794. The experimental study was approved by the Research Ethics Committee of the University (#26116). The procedures for obtaining and isolate the SHED were approved by the Ethics Committee of the Universidade Federal do Rio Grande do Sul (#296/08).

Conflict of Interest The authors declare that they have no conflict of interest.

References

1. Lee BB, Cripps R a, Fitzharris M, Wing PC (2014) The global map for traumatic spinal cord injury epidemiology: update 2011, global incidence rate. Spinal Cord 52:110–116. https://doi.org/10.1038/sc.2012.158
2. Oyinbo CA (2011) Secondary injury mechanisms in traumatic spinal cord injury: a nugget of this multiply cascade. Acta Neurobiol Exp (Wars) 71:281–299
3. Cerqueira SR, Oliveira JM, Silva N a et al (2013) Microglia response and in vivo therapeutic potential of methylprednisolone-loaded dendrimer nanoparticles in spinal cord injury. Small 9:738–749. https://doi.org/10.1002/smll.201201888
4. Casella GTB, Bunge MB, Wood PM (2006) Endothelial cell loss is not a major cause of neuronal and glial cell death following contusion injury of the spinal cord. Exp Neurol 202:8–20. https://doi.org/10.1016/j.expneurol.2006.05.028
5. Nicola F do C, Marques MR, Odorcyk F et al (2017) Neuroprotector effect of stem cells from human exfoliated deciduous teeth transplanted after traumatic spinal cord injury involves inhibition of early neuronal apoptosis. Brain Res 1663:95–105. https://doi.org/10.1016/j.brainres.2017.03.015
6. Seki T, Namba T, Mochizuki H, Onodera M (2007) Clustering, migration, and neurite formation of neural precursor cells in the adult rat hippocampus. J Comp Neurol 502:275–290. https://doi.org/10.1002/cne
7. Beck KD, Nguyen HX, Galvan MD, Salazar DL, Woodruff TM, Anderson AJ (2010) Quantitative analysis of cellular inflammation after traumatic spinal cord injury: Evidence for a multiphasic inflammatory response in the acute to chronic environment. Brain 133:433–447. https://doi.org/10.1093/brain/awp322
8. Burda JE, Sofroniew MV (2014) Reactive gliosis and the multicellular response to CNS damage and disease. Neuron 81:229–248. https://doi.org/10.1016/j.neuron.2013.12.034
9. Ridet JL, Malhotra SK, Privat A, Gage FH (1997) Reactive astrocytes: cellular and molecular cues to biological function. Trends Neurosci 20:570–577. https://doi.org/10.1016/S0166-2236(97)01139-9
10. Sofroniew MV (2009) Molecular dissection of reactive astrogliosis and glial scar formation. Trends Neurosci 32:638–647. https://doi.org/10.1016/j.tins.2009.08.002
11. Saadoun S, Papadopoulos MC (2010) Aquaporin-4 in brain and spinal cord oedema. Neuroscience 168:1036–1046. https://doi.org/10.1016/j.neuroscience.2009.08.019
12. Tait MJ, Saadoun S, Bell BA, Papadopoulos MC (2008) Water movements in the brain: Role of aquaporins. Trends Neurosci 31:37–43. https://doi.org/10.1016/j.tins.2007.11.003
13. Nesic O, Guest JD, Zivadinovic D, Narayana PA, Herrera JJ, Grill RJ, Mokkapati VUL, Gelman BB et al (2010) Aquaporins in spinal cord injury: the janus face of aquaporin 4. Neuroscience 168:1019–1035. https://doi.org/10.1016/j.neuroscience.2010.01.037
14. Butt AM, Kalsi A (2006) Inwardly rectifying potassium channels (Kir) in central nervous system glia: A special role for Kir4.1 in glial functions. J Cell Mol Med 10:33–44. https://doi.org/10.1111/j.1582-4934.2006.tb00289.x
15. Nichols CG, Lopatin a N (1997) Inward rectifier potassium channels. Annu Rev Physiol 59:171–191. https://doi.org/10.1146/annurev.physiol.59.1.171
16. Sibille J, Pannasch U, Rouach N (2014) Astroglial potassium clearance contributes to short-term plasticity of synaptically evoked currents at the tripartite synapse. J Physiol 592:87–102. https://doi.org/10.1113/jphysiol.2013.261735
17. Allaman I, Bélanger M, Magistretti PJ (2011) Astrocyte-neuron metabolic relationships: For better and for worse. Trends Neurosci 34:76–87
18. Donato R, R. Cannon B, Sorci G, et al (2013) Functions of S100 proteins. Curr Mol Med 13:24–57 . doi: https://doi.org/10.2174/156652413804486214
19. Raponi E, Agenes F, Delphin C, Assard N, Baudier J, Legraverend C, Deloulme JC (2007) S100B expression defines a state in which GFAP-expressing cells lose their neural stem cell potential and acquire a more mature developmental stage. Glia 55:165–177. https://doi.org/10.1002/glia.20445
20. Gronthos S, Mankani M, Brahim J, Robey PG, Shi S (2000) Postnatal human dental pulp stem cells (DPSCs) in vitro and in vivo. Proc Natl Acad Sci U S A 97:13625–13630. https://doi.org/10.1073/pnas.240309797
21. Miura M, Gronthos S, Zhao M, Lu B, Fisher LW, Robey PG, Shi S (2003) SHED: Stem cells from human exfoliated deciduous teeth. Proc Natl Acad Sci U S A 100:5807–5812. https://doi.org/10.1073/pnas.0937635100
22. De Berdt P, Bottemanne P, Bianco J, et al (123AD) Stem cells from human apical papilla decrease neuro-inflammation and stimulate oligodendrocyte progenitor differentiation via activin-A secretion. Cell Mol Life Sci 1: . doi: https://doi.org/10.1007/s00018-018-2764-5
23. Nicola FC, Rodrigues LP, Crestani T, Quintiliano K, Sanches EF, Willborn S, Aristimunha D, Boisserand L et al (2016) Human dental pulp stem cells transplantation combined with treadmill training in rats after traumatic spinal cord injury. Brazilian J Med Biol Res = Rev Bras Pesqui medicas e Biol 49:e5319. https://doi.org/10.1590/1414-431X20165319
24. Sakai K, Yamamoto A, Matsubara K, Nakamura S, Naruse M, Yamagata M, Sakamoto K, Tauchi R et al (2012) Human dental pulp-derived stem cells promote locomotor recovery after complete transection of the rat spinal cord by multiple neuro-regenerative mechanisms. J Clin Invest 122:80–90. https://doi.org/10.1172/JCI59251
25. Taghipour Z, Karbalaie K, Kiani A, Niapour A, Bahramian H, Nasr-Esfahani MH, Baharvand H (2012) Transplantation of undifferentiated and induced human exfoliated deciduous teeth-derived stem cells promote functional recovery of rat spinal cord contusion injury model. Stem Cells Dev 21:1794–1802. https://doi.org/10.1089/scd.2011.0408
26. Matsubara K, Matsushita Y, Sakai K, Kano F, Kondo M, Noda M, Hashimoto N, Imagama S et al (2015) Secreted ectodomain of sialic acid-binding Ig-like lectin-9 and monocyte chemoattractant protein-1 promote recovery after rat spinal cord injury by altering macrophage polarity. J Neurosci 35:2452–2464. https://doi.org/10.1523/JNEUROSCI.4088-14.2015
27. Bernardi L, Luisi SB, Fernandes R, Dalberto TP, Valentim L, Bogo Chies JA, Medeiros Fossati AC, Pranke P (2011) The isolation of stem cells from human deciduous teeth pulp is related to the physiological process of resorption. J Endod 37:973–979. https://doi.org/10.1016/j.joen.2011.04.010
28. Luisi S, Barbachan J, Chies J, Filho M (2007) Behavior of human dental pulp cells exposed to transforming growth factor-beta1 and acidic fibroblast growth factor in culture. J Endod 33:833–835. https://doi.org/10.1016/j.joen.2007.04.002
29. Maurmann N, Pereira DP, Burguez D, de S Pereira FDA, Inforçatti Neto P, Rezende RA, Gamba D, da Silva JVL et al (2017) Mesenchymal stem cells cultivated on scaffolds formed by 3D printed PCL matrices, coated with PLGA electrospun nanofibers for use in tissue engineering. Biomed Phys Eng Express 3. https://doi.org/10.1088/2057-1976/aa6308
30. Weeks J, Hart RP (2004) SCI-base: An open-source spinal cord injury animal experimentation database. Lab Anim (NY) 33:35–41
31. Park DY, Mayle RE, Smith RL, Corcoran-Schwartz I, Kharazi AI, Cheng I (2013) Combined transplantation of human neuronal and mesenchymal stem cells following spinal cord injury. Glob Spine J 3:1–6. https://doi.org/10.1055/s-0033-1337118

32. Xavier Acasigua G, Bernardi L, Braghirolli D, Filho M, Pranke P, Medeiros Fossati A (2014) Nanofiber scaffolds support bone regeneration associated with pulp stem cells. Curr Stem Cell Res Ther 9: 330–337. https://doi.org/10.2174/1574888X09666140228123911
33. Basso DM, Beattie MS, Bresnahan JC (1995) A sensitive and reliable locomotor rating scale for open field testing in rats. J Neurotrauma 12:1–21
34. Tramontina F, Leite MC, Cereser K, de Souza DF, Tramontina AC, Nardin P, Andreazza AC, Gottfried C et al (2007) Immunoassay for glial fibrillary acidic protein: Antigen recognition is affected by its phosphorylation state. J Neurosci Methods 162:282–286. https://doi.org/10.1016/j.jneumeth.2007.01.001
35. Leite MC, Galland F, Brolese G, Guerra MC, Bortolotto JW, Freitas R, Almeida LMV, Gottfried C et al (2008) A simple, sensitive and widely applicable ELISA for S100B: methodological features of the measurement of this glial protein. J Neurosci Methods 169: 93–99. https://doi.org/10.1016/j.jneumeth.2007.11.021
36. Heimfarth L, Loureiro SO, Dutra MF, Petenuzzo L, de Lima BO, Fernandes CG, da Rocha JBT, Pessoa-Pureur R (2013) Disrupted cytoskeletal homeostasis, astrogliosis and apoptotic cell death in the cerebellum of preweaning rats injected with diphenyl ditelluride. Neurotoxicology 34:175–188. https://doi.org/10.1016/j.neuro.2012.10.015
37. Weis SN, Pettenuzzo LF, Krolow R, Valentim LM, Mota CS, Dalmaz C, Wyse ATS, Netto CA (2012) Neonatal hypoxia-ischemia induces sex-related changes in rat brain mitochondria. Mitochondrion 12:271–279. https://doi.org/10.1016/j.mito.2011.10.002
38. Encinas JM, Vaahtokari A, Enikolopov G (2006) Fluoxetine targets early progenitor cells in the adult brain. Proc Natl Acad Sci U S A 103:8233–8238. https://doi.org/10.1073/pnas.0601992103
39. Donato R, Sorci G, Riuzzi F, Arcuri C, Bianchi R, Brozzi F, Tubaro C, Giambanco I (2009) S100B's double life: Intracellular regulator and extracellular signal. Biochim Biophys Acta - Mol Cell Res 1793:1008–1022. https://doi.org/10.1016/j.bbamcr.2008.11.009
40. Ellis KM, Carroll DCO, Lewis MD et al (2014) Neurogenic potential of dental pulp stem cells isolated from murine incisors. Stem Cell Res Ther 5:1–13. https://doi.org/10.1186/scrt419
41. Yamamoto S, Yamamoto N, Kitamura T, Nakamura K, Nakafuku M (2001) Proliferation of parenchymal neural progenitors in response to injury in the adult rat. Spinal Cord 127:115–127. https://doi.org/10.1006/exnr.2001.7798
42. Blades DA, Baldwin SA, Broderick R, Scheff SW (1998) Alterations in temporal/spatial distribution of GFAP- and vimentin-positive astrocytes after spinal cord injury contusion with the New York University spinal cord injury device. J Neurotrauma 15:1015–1026
43. Obermair F, Schröter A, Thallmair M (2008) Endogenous neural progenitor cells as therapeutic target after spinal cord injury. Physiology (Bethesda) 23:296–304. https://doi.org/10.1152/physiol.00017.2008
44. Frisén J, Johansson CB, Török C, Risling M, Lendahl U (1995) Rapid, widespread, and longlasting induction of nestin contributes to the generation of glial scar tissue after CNS injury. J Cell Biol 131:453–464. https://doi.org/10.1083/jcb.131.2.453
45. McKeon RJ, Schreiber RC, Rudge JS, Silver J (1991) Reduction of neurite outgrowth in a model of glial scarring following CNS injury is correlated with the expression of inhibitory molecules on reactive astrocytes. J Neurosci 11:3398–3411
46. Ahuja CS, Wilson JR, Nori S, Kotter MRN, Druschel C, Curt A, Fehlings MG (2017) Traumatic spinal cord injury. Nat Rev Dis Prim 3:17018. https://doi.org/10.1038/nrdp.2017.18
47. Wu D, Klaw MC, Connors T, Kholodilov N, Burke RE, Côté MP, Tom VJ (2017) Combining constitutively active Rheb expression and chondroitinase promotes functional axonal regeneration after cervical spinal cord injury. Mol Ther 25:2715–2726. https://doi.org/10.1016/j.ymthe.2017.08.011
48. Xu C, Klaw MC, Lemay M a et al (2015) Pharmacologically inhibiting kinesin-5 activity with monastrol promotes axonal regeneration following spinal cord injury. Exp Neurol 263:172–176. https://doi.org/10.1016/j.expneurol.2014.10.013
49. Faulkner JR (2004) Reactive astrocytes protect tissue and preserve function after spinal cord injury. J Neurosci 24:2143–2155. https://doi.org/10.1523/JNEUROSCI.3547-03.2004
50. Lee SJ, Kim CW, Lee KJ, Choe JW, Kim SE, Oh JH, Park YS (2010) Elevated serum S100B levels in acute spinal fracture without head injury. Emerg Med J 27:209–212. https://doi.org/10.1136/emj.2008.063743
51. Vos PE, Jacobs B, Andriessen TMJC, Lamers KJB, Borm GF, Beems T, Edwards M, Rosmalen CF et al (2010) GFAP and S100B are biomarkers of traumatic brain injury: an observational cohort study. Neurology 75:1786–1793. https://doi.org/10.1212/WNL.0b013e3181fd62d2
52. Do Carmo Cunha J, De Freitas Azevedo Levy B, De Luca BA et al (2007) Responses of reactive astrocytes containing S100?? protein and fibroblast growth factor-2 in the border and in the adjacent preserved tissue after a contusion injury of the spinal cord in rats: Implications for wound repair and neuroregeneration. Wound Repair Regen 15:134–146. https://doi.org/10.1111/j.1524-475X.2006.00194.x
53. Chen J-Q, Zhang C-C, Jiang S-N, Lu H, Wang W (2016) Effects of aquaporin 4 knockdown on brain edema of the uninjured side after traumatic brain injury in rats. Med Sci Monit 22:4809–4819. https://doi.org/10.12659/MSM.898190
54. Hibino H, Inanobe A, Furutani K, Murakami S, Findlay I, Kurachi Y (2010) Inwardly rectifying potassium channels: their structure, function, and physiological roles. Physiol Rev 90:291–366. https://doi.org/10.1152/physrev.00021.2009
55. Becker D, Sadowsky CL, McDonald JW (2003) Restoring function after spinal cord injury. Neurologist 9:1–15
56. Nesic O, Lee J, Ye Z, Unabia GC, Rafati D, Hulsebosch CE, Perez-Polo JR (2006) Acute and chronic changes in aquaporin 4 expression after spinal cord injury. Neuroscience 143:779–792. https://doi.org/10.1016/j.neuroscience.2006.08.079
57. Nagelhus E a, Mathiisen TM, Ottersen OP (2004) Aquaporin-4 in the central nervous system: cellular and subcellular distribution and coexpression with KIR4.1. Neuroscience 129:905–913. https://doi.org/10.1016/j.neuroscience.2004.08.053
58. Olsen ML, Campbell SC, McFerrin MB et al (2010) Spinal cord injury causes a wide-spread, persistent loss of Kir4.1 and glutamate transporter 1: Benefit of 17??-oestradiol treatment. Brain 133: 1013–1025. https://doi.org/10.1093/brain/awq049
59. Basso DM, Beattie MS, Bresnahan JC (1995) A sensitive and reliable locomotor rating scale for open field testing in rats. J Neurotrauma 12:1–21. https://doi.org/10.1089/neu.1995.12.1
60. Rodrigues LP, Iglesias D, Nicola FC, Steffens D, Valentim L, Witczak A, Zanatta G, Achaval M et al (2012) Transplantation of mononuclear cells from human umbilical cord blood promotes functional recovery after traumatic spinal cord injury in Wistar rats. Brazilian J Med Biol Res 45:49–57. https://doi.org/10.1590/S0100-879X2011007500162
61. de Almeida FM, Marques SA, Ramalho BDS, et al (2011) Human dental pulp cells: a new source of cell therapy in a mouse model of compressive spinal cord injury. J Neurotrauma 28:1939–1949 . doi: https://doi.org/10.1089/neu.2010.1317